SUPPLEMENTAL MATERIAL

Johannes Riegler, PhD[1,2]; Astrid Gillich, PhD[3]; Qi Shen, MS[1,2]; Joseph D. Gold, PhD[3]; Joseph C. Wu, MD, PhD[1,2]

[1]Department of Medicine, Division of Cardiology, [2]Department of Radiology and Stanford Cardiovascular Institute, [3]Department of Biochemistry, [4]Department of Cardiothoracic Surgery, Stanford University School of Medicine, Stanford, CA 94305, USA

SUPPLEMENTAL METHODS

Generation of Cardiac tissue slices (CTS). Cardiac tissue slices were generated similar to a previously described procedure[1]. Adult (8-12 weeks, male and female, n=40) transgenic mice (referred to as L2G) bred on FVB background expressing enhanced green fluorescent protein (eGFP) and firefly luciferase (Fluc) reporter genes driven by a β-actin promoter as previously described[2] were anesthetized using isoflurane. Cuts into were made the liver and hearts were perfused with 10 ml ice-cold modified Tyrode solution (see below) containing 500 international units of heparin per milliliter (Sigma, St. Louis, MO) through the apex with a 25G butterfly needle. Hearts were excised and their right ventricle and all atria were removed to increase mechanical stability during sectioning. The left ventricular lumen was filled through the aorta with 4% low melting point agarose (Invitrogen, Carlsbad CA) using a 20G needle. Hearts were embedded in 4% low melting point agarose in a 30 mm dish and placed on ice. The solidified block was trimmed and glued onto a sample holder of a vibratome (The Vibratome Company, St. Louis, MO) using cyanoacrylate glue. The entire block was covered with ice-cold modified Tyrode solution during the sectioning process. Sections with different thicknesses (100 – 800 μm) were cut from the left ventricular free wall. To standardize the slices, discs with a diameter of 3 or 5 mm were punched out using core sample punchers (Fine Science Tools, Foster City, CA) and stored in modified Tyrode solution until transplantation or other use (see Figure 1A). Skeletal muscle patches from the thigh (vastus lateralis) were generated from L2G mice using a similar procedure. Skeletal muscle patches were cut in parallel to the primary fiber orientation of the muscle tissue.

Modified Tyrode solution. The following chemicals (Sigma, St. Louis, MO) were dissolved in distilled water: 136 mmol/l NaCL, 5.4 mmol/l KCl, 1 mmol/l $MgHPO_4 \cdot 3H_20$, 10 mmol/l D-

Glucose, 0.09 mmol/l $CaCl_2$, 30 mmol/l 2,3-Butanedione monoxime, and 5 mmol/l HEPES. The pH was adjusted to 7.4 and the solution was sterile filtered.

Assessing cell death due to vibratome sectioning. CTS from adult L2G mice were prepared with a thickness of 250 μm and stored in Tyrode solution for 4 hours. CTS were fixed for 20 minutes in 4% PFA. Some CTS were used for whole mount confocal microscopy while others were frozen in OCT, sectioned and used for TUNEL staining (see below). Confocal microscopy was performed using a Leica SP5 microscope (Leica, Wetzlar, Germany). A series of images was acquired with a 20x glycerol immersion objective with a zoom factor of 1.4. A z-stack (60 slices) was acquired for whole mount CTS to generate 3D renderings of the vibratome cutting surface.

Myocardial infarction and CTS transplantation. MI was induced in male NOD/SCID mice (Charles River Laboratories, Wilmington, MA) by permanent LAD ligation under 1.5% to 2% inhaled isoflurane after left thoracotomy and confirmed by myocardial blanching and ECG changes. Animals were randomized into experimental groups receiving either CTS (n=36), skeletal muscle patches (n=12), or control group receiving no patch (n=12). For all experiments involving cardiac assessment via magnetic resonance imaging (MRI), CTS and skeletal muscle patches with 5 mm diameter and 400 μm thickness were transplanted directly after LAD occlusion. CTS and skeletal muscle patches were attached onto the left ventricular (LV) free wall with 4-5 stitches using 10-0 silk sutures. For patch survival and reperfusion experiments, CTS with 3 mm diameter were transplanted onto the LV free wall of non-infarcted mice (n=52, NOD/SCID). All surgeries were performed by experienced microsurgeons. Mice received antibiotics via their drinking water from the surgery day on until the end of the experiment.

Origin of FSP1 positive cells found in the graft following transplantation. CTS were made from adult hearts of Sox2-Cre; Rosa26-tdTomato double heterozygous mice (n=6) (C57BL/6 background) with permanent labelling of cells with tdTomato. These tdTomato positive CTS were transplanted onto non-infarcted mouse hearts (n=12, NOD/SCID). Three hearts where harvested on day 1, 3, 6 and 9 after CTS transplantation as outlined below.

Assessment of endothelial cell origin in reperfused CTS. CTS were transplanted as described above onto non-infarcted hearts of adult VE-cadherin-Cre; Rosa26-tdTomato double heterozygous mice (n=18) (C57BL/6 background) with specific and permanent labeling of endothelial cells with tdTomato. To prevent immune rejection, Tacrolimus (5 mg/kg/day Astellas, Northbrook, IL) was orally administered every 12 hours starting one day before CTS transplantation. Mice received antibiotics via their drinking water throughout the experiment.

Survival of neonatal cardiac tissue slices. Neonatal pups from L2G mice (1 day old) were sacrificed, their hearts excised and placed into ice-cold modified Tyrode solution. Hearts were cut longitudinally and patches were punched out of the left ventricular free wall (approx. 3 mm diameter) and transplanted onto infarcted (n=5) or control (n=5) NOD/SCID mice as described above. The slices were not always entirely circular due to the small size of the left ventricular free wall of neonatal hearts.

Bioluminescence imaging (BLI). Mice were anesthetized with isoflurane, D-Luciferin (400 mg/kg, Biosynth International, Itasca, IL) was injected intraperitoneally, and mice were placed into a BLI imaging system (Xenogen, Alameda, CA). Images were acquired every two minutes until a stable decline in signal intensity could be observed. Regions of interest (ROI) were placed

over the chest centred at the pixel with maximum signal intensity. The ROI with the maximum of the average signal intensity from all the ROIs of one time series belonging to one animal was selected as measurement value for that imaging session. The ROI size was kept constant for all animals and experiments. In order to get a better estimate of the number of transplanted cells, the first BLI time point was always 4 hours after transplantation surgery.

Estimating cell survival using BLI. Human embryonic stem (hESCs) were transduced with a Fluc-eGFP double fusion construct by lentivirus-based techniques as previously described[3]. Undifferentiated hESCs (H7 line from Wicell) were grown and expanded on Matrigel-coated plates in mTeSR1 medium (Stem Cell Technologies, Vancouver, BC, Canada). ESCs were detached using Trypsin and filtered through a 50 μm pore size filter to avoid cell clumps. The number of viable cells was estimated using Trypan blue exclusion with an automatic cell counter (Countess, Invitrogen, Carlsbad, CA). Cells were diluted and plated in 200 μl media at varying concentrations (2.5E5, 6.2E4, 1.5E4, 4E3) in wells of a 96 well plate. D-Luciferin (0.05 mg/well, Biosynth International, Itasca, IL) was added and the radiance was measured immediately afterwards using the same BLI imaging system used for mice. The experiment was repeated once.

Immunodetection and histological methods

Heart fixation and section preparation: Mice were anesthetized, cuts into the liver were made and their hearts were perfused with 10 ml cold PBS (4 ºC) containing 0.1 mol/l KCl through a 25G butterfly needle inserted into the left ventricle via the apex. Hearts were cut out and fixed over night at 4 ºC in PBS with 4% PFA. Following fixation, hearts were placed into PBS for four hours before whole heart fluorescence images were acquired (CRi Maestro, Perkin

Elmer, Waltham, MA). After that, hearts were transferred into 30% sucrose solution and kept at 4 ºC until equilibrium was reached. Hearts were embedded in OCT and frozen in hexane containing dry ice. Sections were cut with a cryostat (Leica, Wetzlar, Germany) collected on glass slides, dried and stored at -80 ºC.

Cell death: TUNEL staining was performed on 8 µm thick cryosections using a commercial kit (Roche, Mannheim, Germany) following the manufacturer's instructions except for the following modifications. Sections were permeabilized in 0.1 M citric acid at 65 ºC for 30 minutes. The TUNEL reaction mixture was diluted 1:4 with TUNEL dilution buffer. After TUNEL staining, sections were washed 3x 10 minutes with PBS and a standard immunofluorescence staining procedure followed.

Immunofluorescence: Sections were equilibrated to room temperature, washed 3x 10 min with PBS, permeabilized with 0.5% Triton-X (Sigma) in PBS for 30 minutes at room temperature followed by incubation in blocking solution (5% donkey serum in PBS + 0.1% Tween20, Sigma) for 30 minutes. For mouse primary antibodies, a mouse-on-mouse blocking kit was used following the manufacturer's instructions (Vector Labs, Burlingame, CA). Sections were incubated with primary antibodies (see Supplemental Table 2) diluted in blocking solution over night at 4 ºC in a humid chamber. After washing 3x 15 min with PBS + 0.1% Tween20, sections were incubated with secondary antibodies diluted in blocking solution for 1 hour followed by a final washing step (3x 15 min in PBS + 0.1% Tween20) and covered with cover slips using self-hardening mounting media. Confocal microscopy was performed using a Leica SP5 microscope (Leica, Wetzlar, Germany). A series of images was acquired with a 40x oil immersion objective. Images were stitched together to generate composite images for further analysis (typically 30-40 individual field of views).

Image analysis: Composite images were analysed using Volocity (PerkinElmer, Waltham, MA). Automatic segmentation of nuclei was performed followed by automatic detection of stained objects at respective channels. A region of interest was manually drawn to limit the analysis to the graft. Endothelial cells, FSP1 positive or CD45 positive cells were identified via colocalization of DAPI stained nuclei with detected objects (for example objects in the far red channel for FSP1 stained with Alexa Flour 647 secondary antibody). For cardiomyocytes, a manual segmentation was performed to designate inside cardiac troponin T or alpha actinin positive cells as cardiomyocyte nuclei. Apoptotic cells were detected by automatic segmentation of TUNEL positive nuclei and colocalization with DAPI positive nuclei. For each animal, 8,000-12,000 graft nuclei were analyzed.

Reperfusion experiments: To assess if blood vessels were perfused, mice were injected intravenously with biotinylated tomato lectin (10 mg/kg, Jackson ImmunoResearch, Baltimore, PA) 15 minutes before they were sacrificed. Heart fixation and immunofluorescence was performed as described above with fluorescently labeled streptavidin (see Supplemental Table 2).

Magnetic resonance imaging (MRI). Imaging was performed using a preclinical 7T (MR901 Discovery) horizontal bore scanner (Agilent, Santa Clara, CA) with a shielded gradient system (600 mT/m). Mice were anaesthetised with isoflurane (3%) and placed onto an animal cradle in prone position. Animals were kept at 37±0.4 °C (during image acquisition) via an air heating system while oxygen and anaesthetics (1-2% isoflurane) were supplied via a nose cone (0.5 L/min). Data acquisition was performed with a 30 mm Millipede transmit/receive volume coil (Agilent). Long and short axis scout images were acquired to define the two and four chamber long axis views. The cine long-axis views were used to define the short axis orientation. A

prospectively double gated (ECG and respiration) spoiled gradient echo sequence was used to acquire cine cardiac images with the following parameters for standard cine acquisitions: TE 1.3 ms, TR 5-6 ms, flip angle 15°, slice thickness 1 mm, no slice separation, FOV 25×25 mm², matrix size 192×192, NSA 3. Twenty cine-frames were recorded to cover the cardiac cycle. A single short-axis slice was obtained in approximately 90 seconds, leading to a total scan time of 11 to 15 minutes covering the apex to base (8-11 slices). For infarct size measurements, late gadolinium enhancement (LGE) images were acquired 15 min after i.p. injection of gadolinium (0.6 mmol/kg, Magnevist Bayer, Germany) using an inversion recovery gradient echo sequence with inversion time optimised to null the healthy myocardium.[4] All images from one animal were combined to a dataset, randomized, and anonymised. Data analysis was performed using the semi-automatic segmentation software Segment (Medviso AB, Sweden)[5] as previously described.[6]

Supplemental Table 1: Cardiac MRI of control, CTS, and muscle patch groups

	Day 1			Day 28		
	Control (n=12)	CTS (n=12)	Muscle patch (n=11)	Control (n=12)	CTS (n=12)	Muscle patch (n=6)
Body weight [g]	21.9 ± 3.6	22.3 ± 3.8	24.0 ± 1.1	22.6 ± 3.4	23.4 ± 3.6	25.4 ± 2.1
Heart rate [bmp]	565 ± 39	564 ± 48	548 ± 31	555 ± 41	555 ± 34	560 ± 20
EDV [µl]	40.2 ± 8.8	43.0 ± 11.8	52.7 ± 6.2*	98.3 ± 23.9	90.4 ± 24.1	123.4 ± 31*
ESV [µl]	24.7 ± 5.3	27.2 ± 9.8	33.0 ± 8.1*	78.5 ± 23.6	66.2 ± 23.2	101.2 ± 32*
SV [µl]	15.5 ± 5.7	15.9 ± 3.4	19.7 ± 3.2	19.9 ± 4.9	24.2 ± 3.2	22.2 ± 3.3
EF [%]	38.0 ± 8.7	37.9 ± 7.4	38.1 ± 8.7	21 ± 6.1	28.3 ± 7.9*	19.2 ± 6.5
CO [ml/min]	8.7 ± 3.2	8.9 ± 1.6	10.7 ± 1.5	11.0 ± 2.8	13.4 ± 2.0	12.4 ± 1.9
LVM [mg]	66.3 ± 11.9	70.1 ± 13.0	72.4 ± 4.6	68.7 ± 9.8	66 ± 10.8	74.9 ± 6.4
Scar [µl]	15.5 ± 3.6	16.9 ± 4.9	17 ± 4.4			
Infarct [% of LVM]	25.1 ± 4.5	25.4 ± 6.2	24.6 ± 6	* $p<0.05$ vs. control		

Data: Mean ± SD

Supplemental Table 2: List of antibodies

Antibody	**Dilution**	**Vendor**	**Order Nr.**
Streptavidin-Cy3	1:600	Invitrogen	43-4315
Donkey secondary antibodies	1:200	Jackson ImmunoResearch	
Connexin 43	1:300	Sigma	C6219-.2ML
FSP1/S100A4	1:200	Millipore	07-2274
cardiac Troponin T	1:100	Thermo Scientific	MS-295-P0
CD31 (Pecam1)	1:200	BD Biosciences	550274
α-Actinin	1:100	Sigma	A7811-.2ML
α-smooth muscle actin	1:500	Sigma	C6198-.2ML
CD45	1:200	Millipore	05-1416
skeletal myosin heavy chain	1:50	Abcam	ab91506

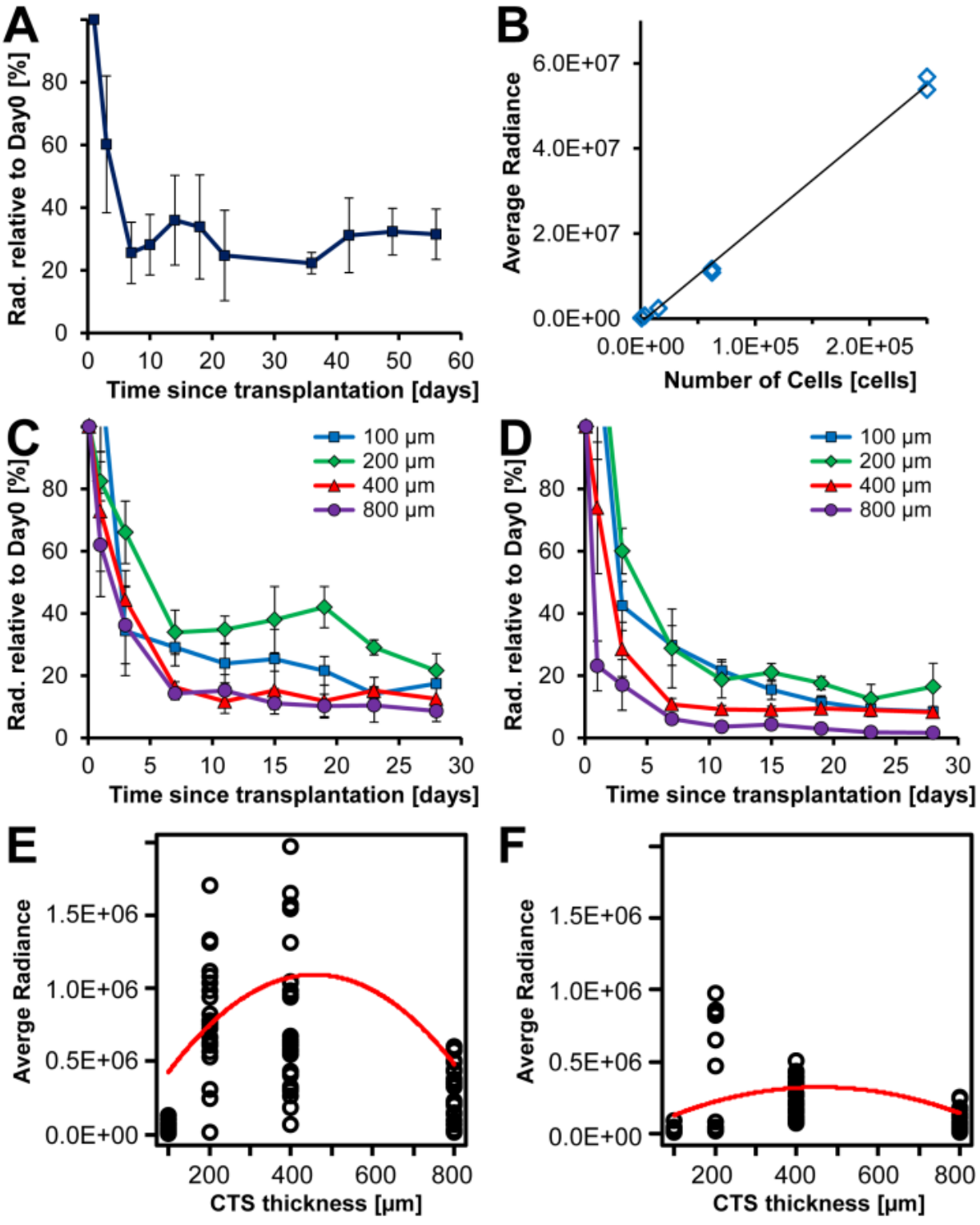

Supplemental Figure I

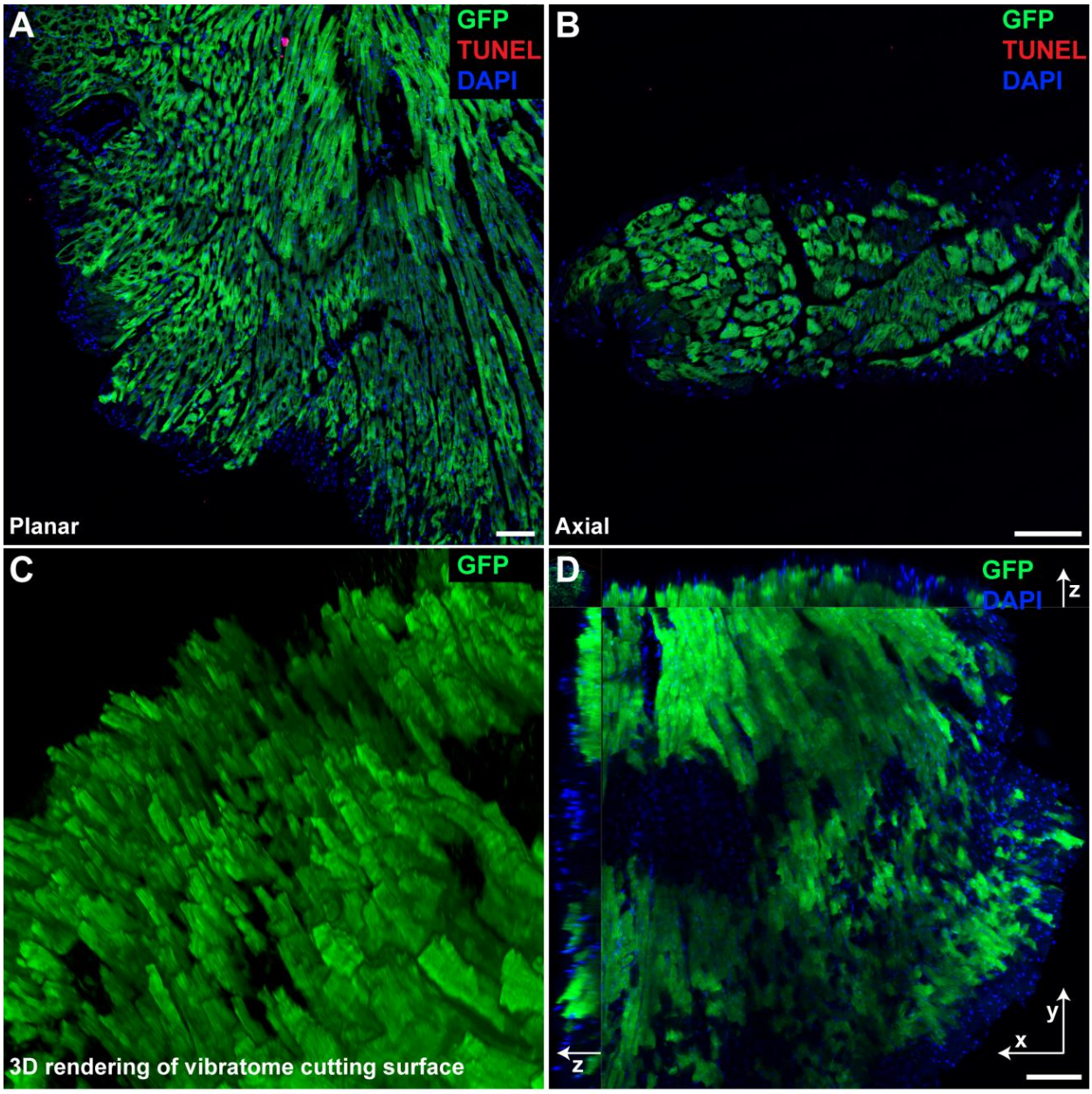

Supplemental Figure II

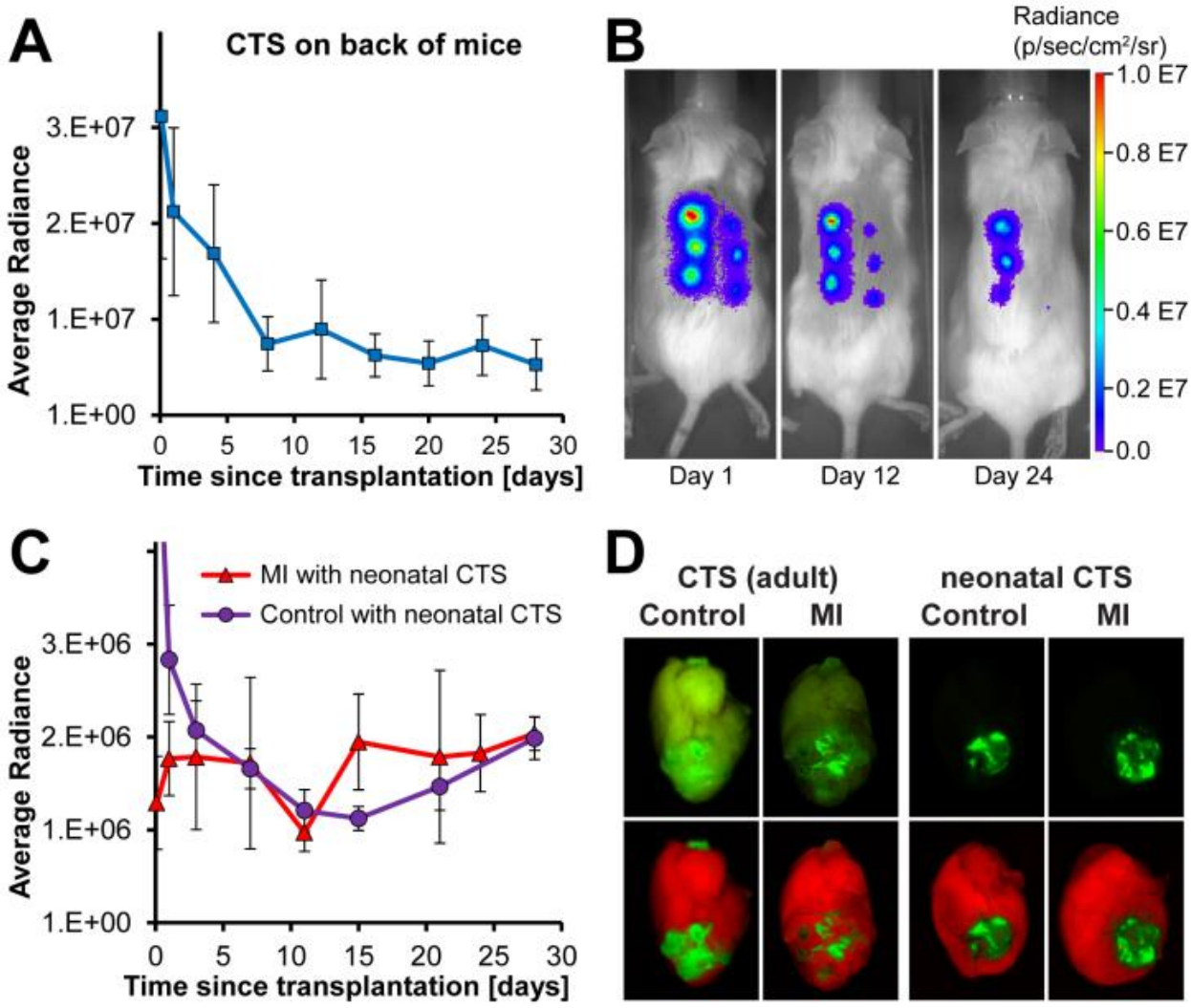

Supplemental Figure III

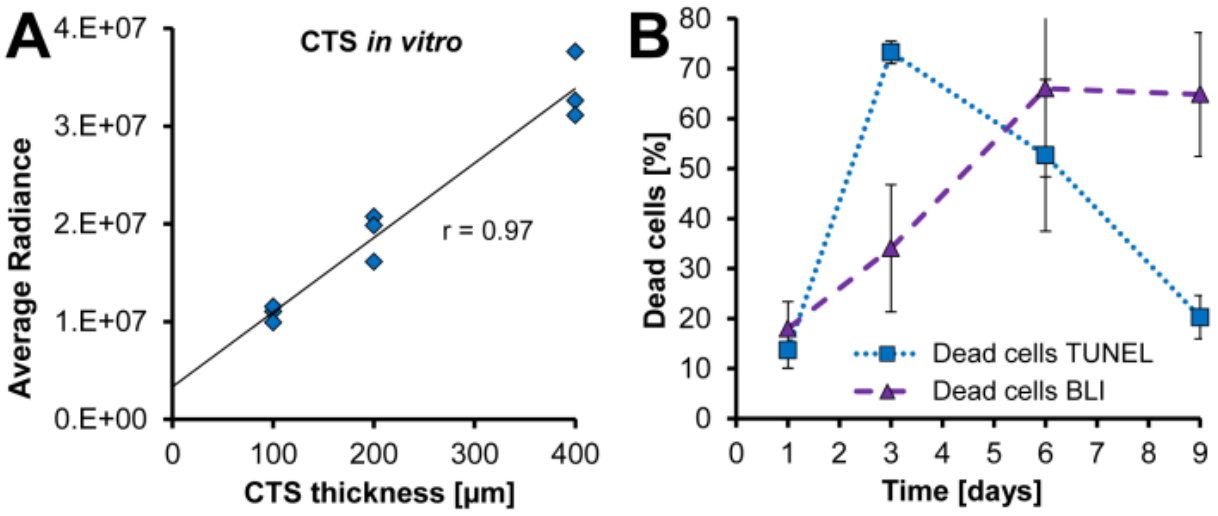

Supplemental Figure IV

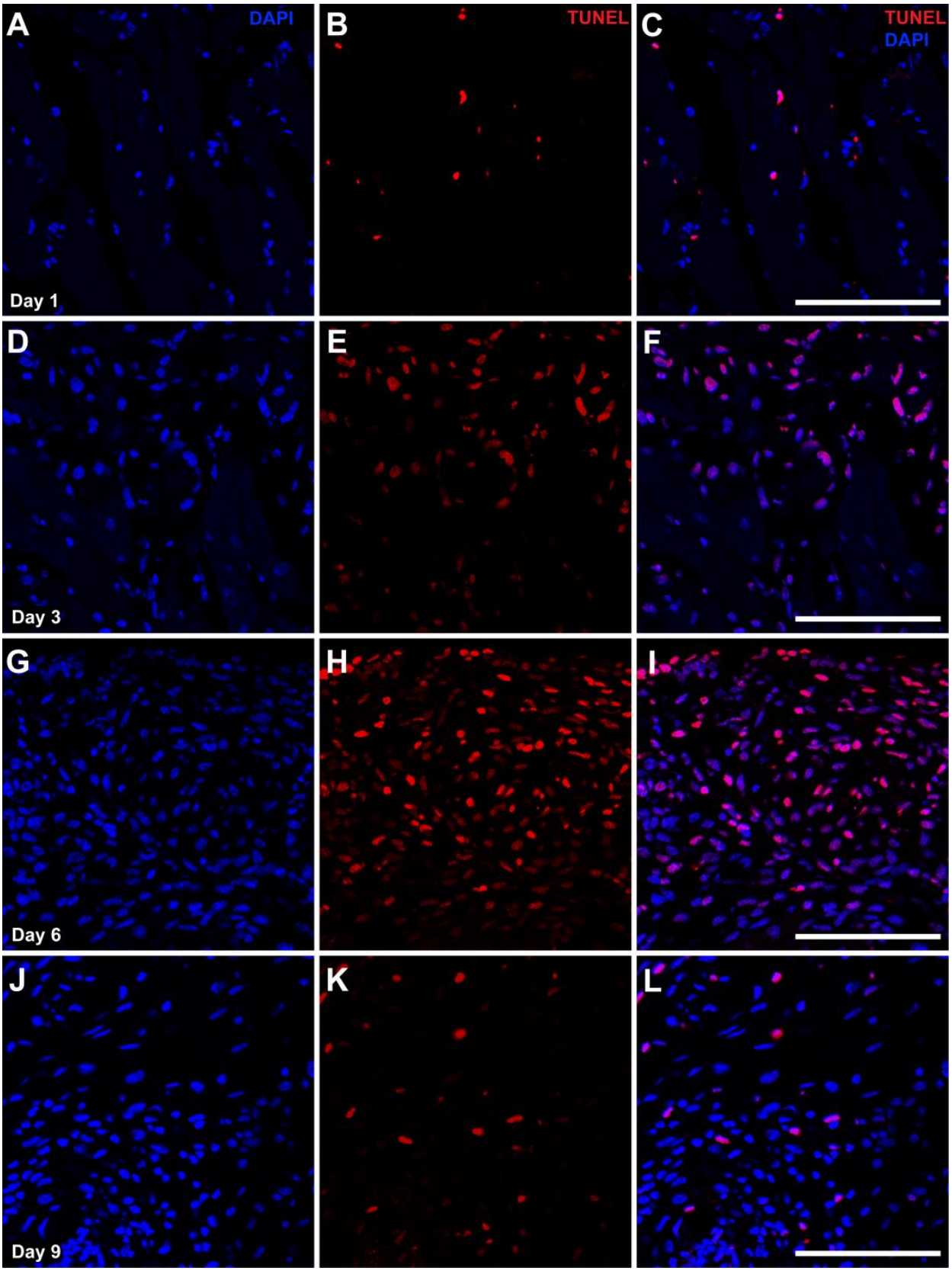

Supplemental Figure V

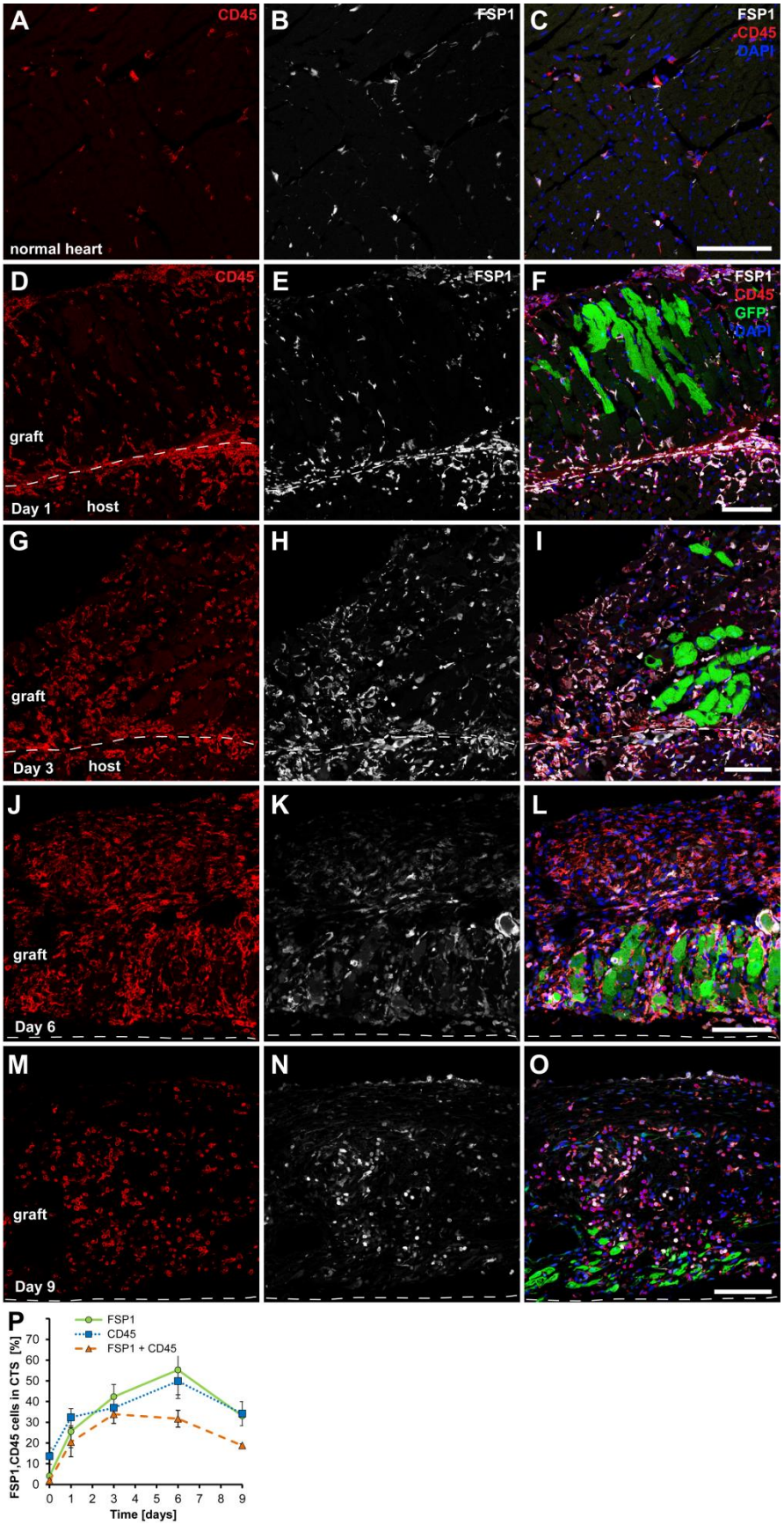

Supplemental Figure VI

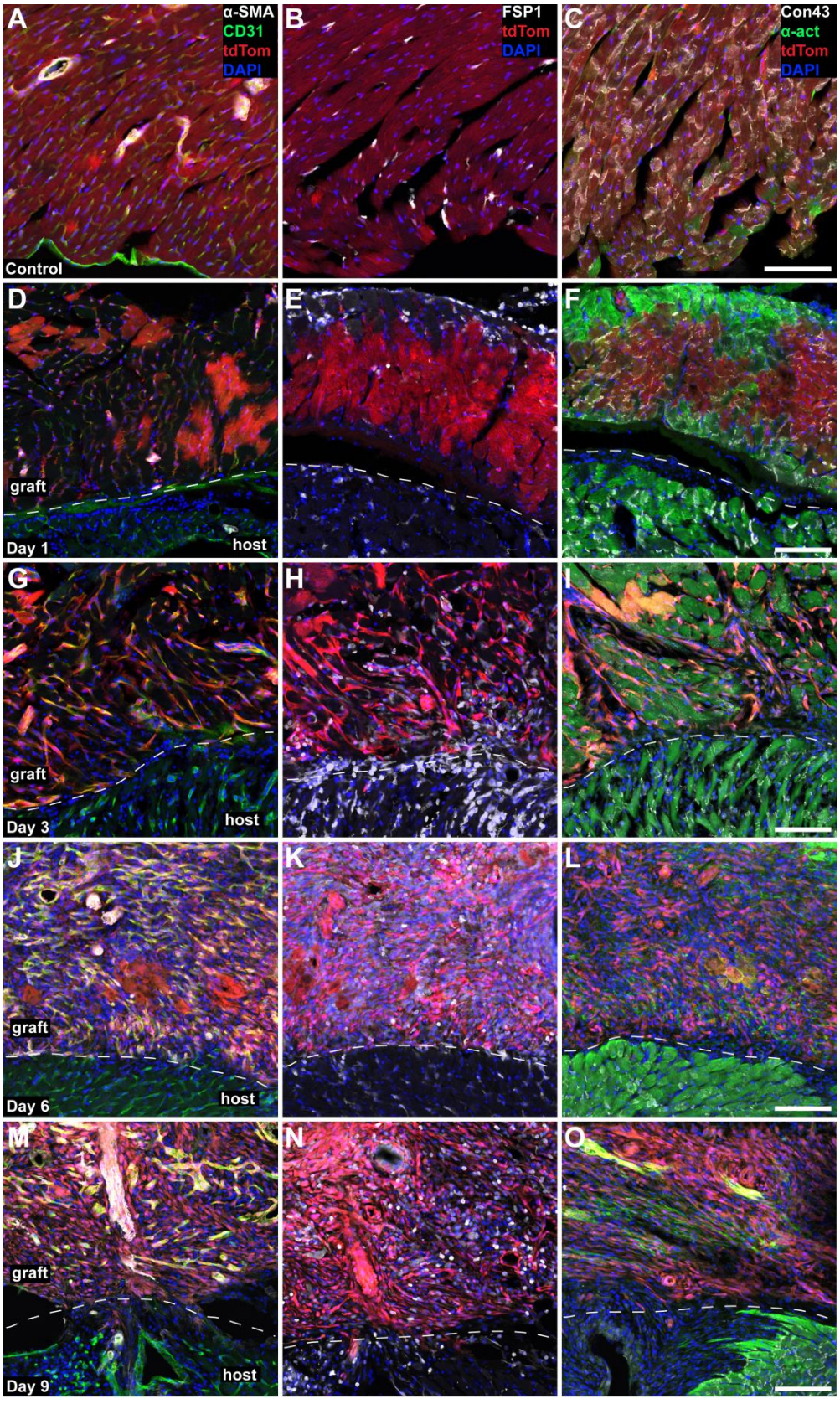

Supplemental Figure VII

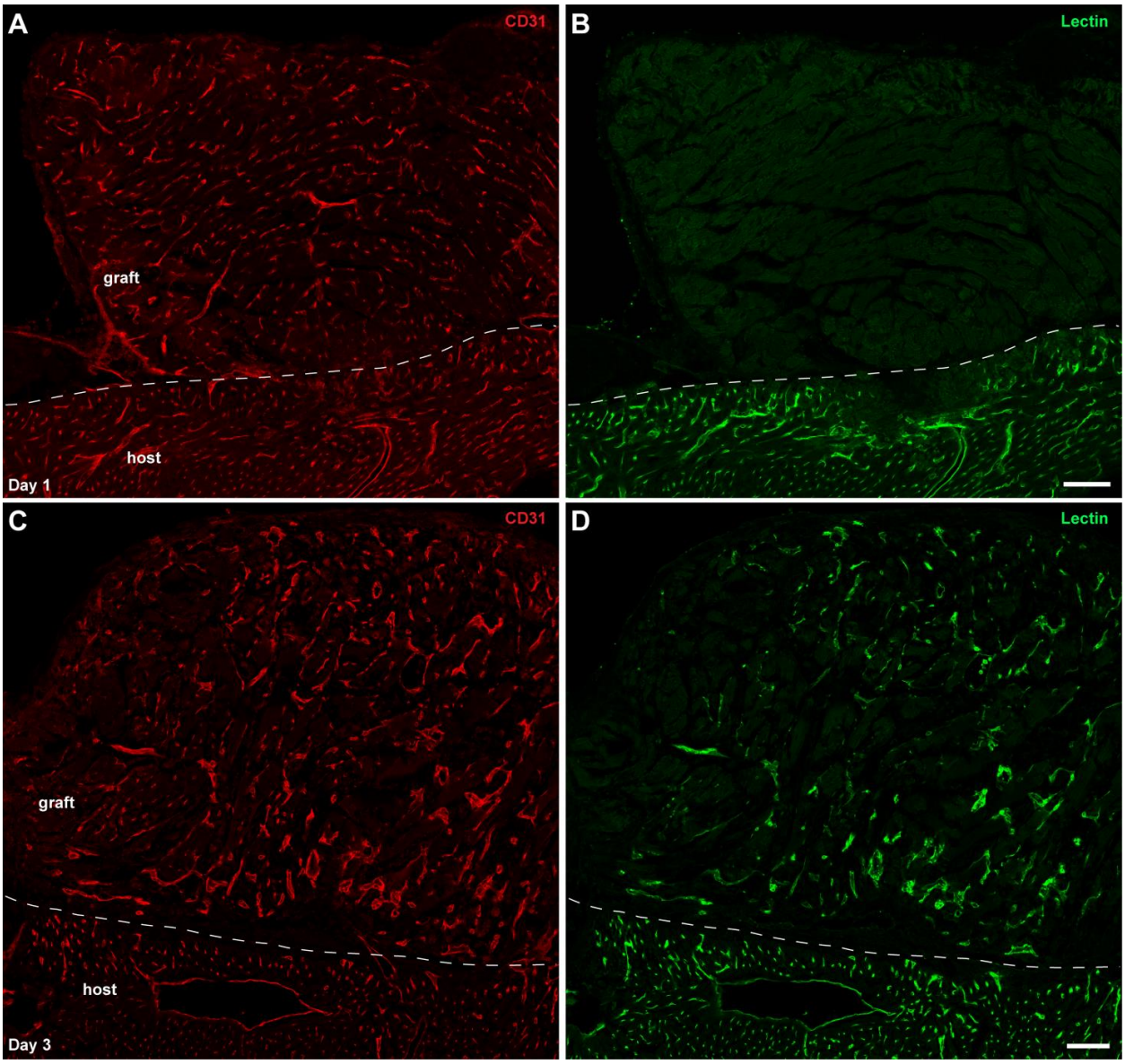

Supplemental Figure VIII

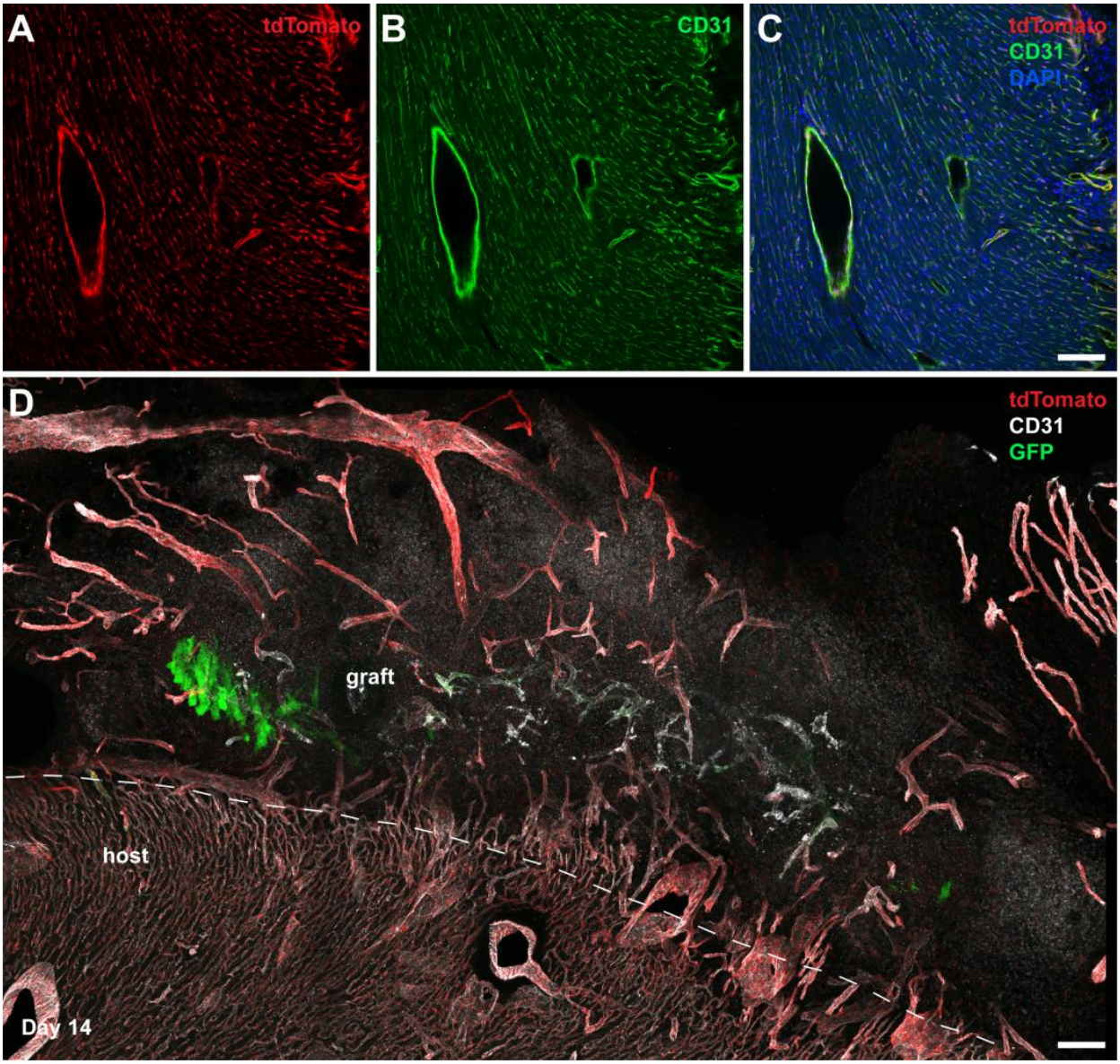

Supplemental Figure IX

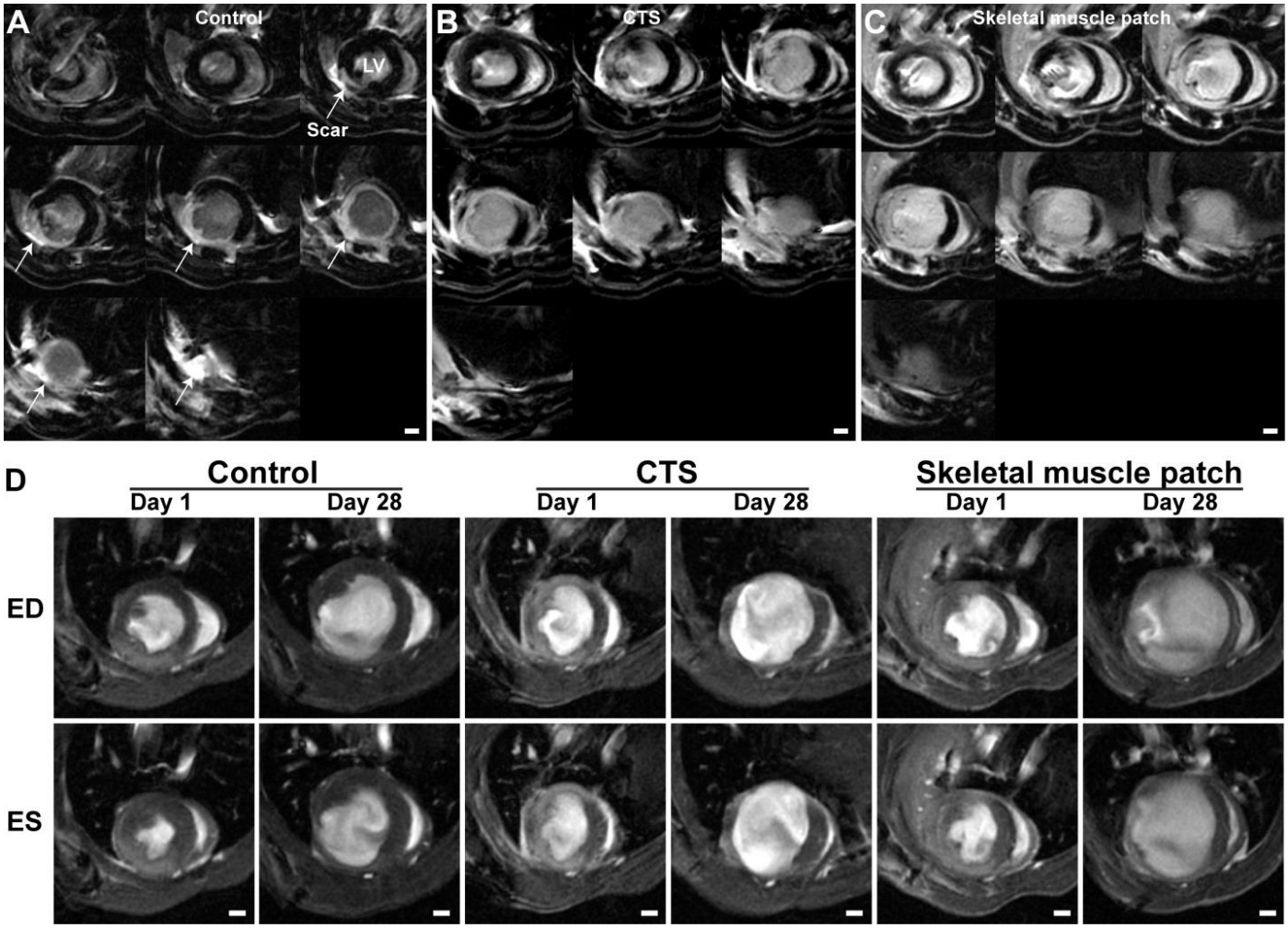

Supplemental Figure X

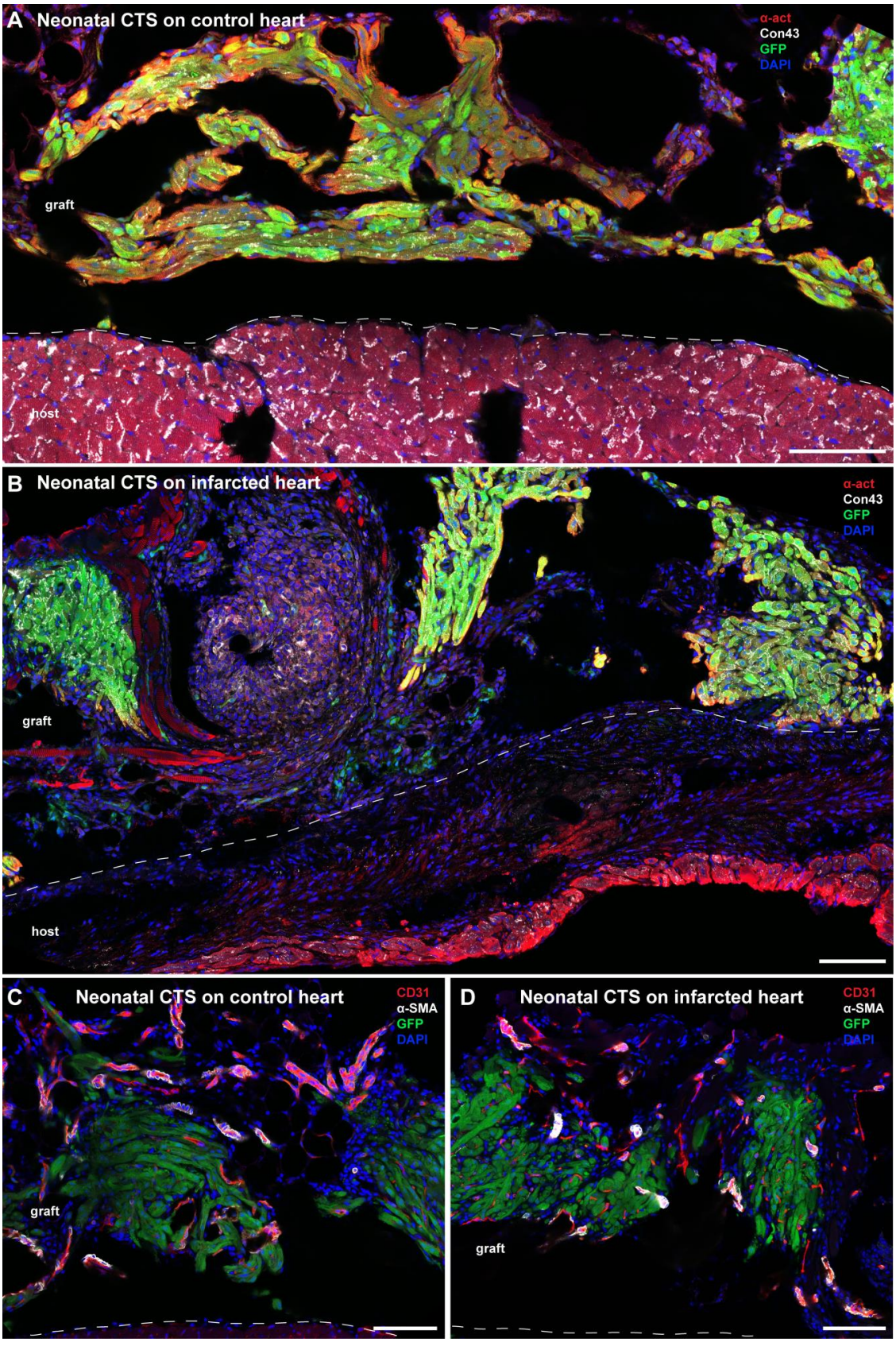

Supplemental Figure XI

SUPPLEMENTAL FIGURE LEGENDS

Supplemental Figure I: Estimating cell survival with Bioluminescence imaging. (**A**) Radiance of transplanted CTS relative to initial signal. (**B**) Linear regression between number of viable cells and average radiance per well indicating BLI can be used as a surrogate for cell viability. (**C**) Radiance relative to day 0 for CTS with different thicknesses transplanted onto normal hearts. (**D**) Radiance relative to day 0 for CTS with different thicknesses transplanted onto infarcted hearts. (**E**) A model with a linear and a quadratic term for CTS thickness was fitted to the BLI data (day 7-28) to illustrate diffusion limited survival on normal mouse hearts. (**F**) The same quadratic model was used to fit the data for CTS transplanted onto infarcted hearts. Average radiance is expressed as photons/second/cm²/steradian. Rad: Radiance.

Supplemental Figure II: *In vitro* characterisation of cardiac tissue slices. (**A, B**) Cardiac tissue slices from adult L2G (GFP positive) mice were generated and kept in Tyrode solution for four hours before they were processed. TUNEL staining did not label many cells, which was probably due to insufficient time to generate enough DNA double strand breaks in mechanically damaged cells. However, cytoplasmic GFP was lost from cells along the cutting surfaces indicating that these cells are likely to be dead. (**C**) Three dimensional projection of the vibratome cutting surface which shows cardiomyocytes are primarily separated along their cell boundaries. (**D**) Z-stack of corresponding images for panel C. Scale bars: 100 µm.

Supplemental Figure III: Survival of cardiac tissue slices transplanted onto the back of mice and survival of neonatal cardiac tissue slices transplanted onto control or MI hearts. **(A)** Adult CTS transplanted subcutaneously onto the back of mice showed survival kinetics similar to adult CTS transplanted onto hearts, illustrating that the observed survival is not

specific to the cardiac microenvironment. **(B)** Representative BLI of adult CTS transplanted onto the back of mice (the right row of CTS had thickness of 100 µm, the left row 300 µm). (**C**) Neonatal CTS transplanted onto normal or infarcted hearts demonstrated similar cell survival one month after transplantation. (**D**) This was also evident on whole heart fluorescence images before (top row) and after spectral decomposition (bottom row). Average radiance is expressed as photons/second/cm²/steradian.

Supplemental Figure IV: Bioluminescence signal intensity for different CTS thicknesses and comparison of cell death estimates by BLI and TUNEL. (**A**) A linear correlation between CTS thickness and average BLI signal intensity was found for CTS, indicating the suitability of BLI to assess graft survival. (**B**) BLI imaging showed a loss of signal intensity for the first week after transplantation. A qualitatively similar behaviour was found for $TUNEL^+$ cells which reached their highest level between day three and six after transplantation and declined thereafter.

Supplemental Figure V: Cell death in transplanted CTS peaked at day six after transplantation. (**A-C**) Nuclei stained with DAPI (blue), apoptotic nuclei which stained TUNEL positive (red) and merged images. Only a small amount of dead cells could be found one day after transplantation. (**D-I**) The number of dead cells increased on day three and reached its maximum on day six. (**J-L**) On day nine after transplantation, the number of dead cells did decrease substantially. All the images in this figure a smaller subsections from the first column of Figure 2. Scale bars: 100 µm.

Supplemental Figure VI: A high number of FSP1 positive cells in transplanted CTS stain positive for the pan-leukocyte marker CD45. (**A-C**) Healthy myocardium contains a small number of pan-leukocytic cells ($CD45^+$) some of which are also FSP1 positive. (**D-L**) The percentage of $CD45^+$ cells as well as the percentage of $FSP1^+$ and $CD45^+$ cells increases rapidly from the first day after CTS transplantation and peaked at day six. (**P**) However, the percentage of double positive cells levelled out from day three onward. Scale bars: 100 µm.

Supplemental Figure VII: The number of fibroblasts and pan-leukocytic cells in CTS increased for the first few days following transplantation primarily via infiltration from the host. (**A-C**) Cardiac tissue from adult Sox2-Cre; Rosa26-tdTomato double heterozygous mice showed uniform tdTomato labelling. (**D-F**) One day after transplantation, CTS labelling was less uniform and a small increase of $FSP1^+$ cells on the edges of the graft was observed. (**G-I**) Three and six days after transplantation, an increase of $FSP1^+$ cells in the graft was observed. A considerable fraction of these cells was tdTomato negative and most likely of host origin. (**M-O**) Nine days after transplantation, grafts still had many blood vessels ($CD31^+$) and a lower amount of $FSP1^+$ cells. However, the number of cardiomyocytes (α-act: α-$actinin^+$) had also declined. α-SMA: alpha smooth muscle actin; tdTom: tdTomato; FSP1: fibroblast specific protein 1; Con43: Connexin 43; Scale bars: 100 µm.

Supplemental Figure VIII: Spatial heterogeneity of reperfused vessels in the CTS grafts three days after transplantation. (**A, B**) CTS grafts had a normal vasculature density one day after transplantation onto control mice hearts; these vessels were not perfused since no intravenous injected lectin was detected in the graft. (**C**, **D**) Three days after transplantation, a

fraction of theses vessel was reperfused although the extent was spatially heterogeneous. Scale bars: 100 µm.

Supplemental Figure IX: CTS grafts were also revascularized via blood vessels from surrounding tissue. (**A-C**) All endothelial cells were tdTomato positive in the linage labelled mice used for these experiments. (**D**) Blood vessels from the host heart growing into CTS grafts were observed in all animals. However, some animals also had vessels growing into the graft from surrounding tissue (maximum intensity projection, 50 slices with one µm slice thickness). Scale bars: 100 µm

Supplemental Figure X: Representative MRI showing similar scar sizes between groups and strong dilative remodelling in the skeletal muscle patch group. (**A-C**) Representative short-axis late gadolinium enhancement MRI from base to apex showing that CTS or skeletal muscle patch transplantation did not alter the infarct size (scar size). The arrows in the control heart point to the gadolinium enhanced infarct scar. (**D**) Representative mid ventricular short-axis views illustrate dilative remodelling between day one and 28 in mice receiving no treatment: control, CTS, or skeletal muscle patch transplants. The top row shows hearts at end-diastole (ED) on day one and 28 while the bottom row depicts the same hearts at end-systole (ES). LV: left ventricle; Scale bars: 1 mm

Supplemental Figure XI: Neonatal CTS survive equally well when transplanted onto control or infarcted hearts. (**A**) Grafts from neonatal CTS contained a substantial number of cardiomyocytes (α-act^{+}: α-actinin) one month after transplantation onto control hearts. (**B**) When neonatal CTS were transplanted onto infarcted hearts, a similar amount of surviving

cardiomyocytes was found one month after transplantation. (**C, D**) The number of capillaries ($CD31^+$) and arteries ($CD31^+$ + α-SMA^+: α-smooth muscle actin) in grafts one month after transplantation of neonatal CTS onto either control or infarct hearts was similar. GFP: green fluorescent protein (graft), Con43: connexion 43, Scale bars: 100 µm

SUPPLEMENTAL REFERENCES

1. Brandenburger M, Wenzel J, Bogdan R, Richardt D, Nguemo F, Reppel M, Hescheler J, Terlau H, Dendorfer A. Organotypic slice culture from human adult ventricular myocardium. *Cardiovasc Res*. 2012;93:50-59
2. Cao YA, Wagers AJ, Beilhack A, Dusich J, Bachmann MH, Negrin RS, Weissman IL, Contag CH. Shifting foci of hematopoiesis during reconstitution from single stem cells. *Proc Natl Acad Sci U S A*. 2004;101:221-226
3. Pearl JI, Lee AS, Leveson-Gower DB, Sun N, Ghosh Z, Lan F, Ransohoff J, Negrin RS, Davis MM, Wu JC. Short-term immunosuppression promotes engraftment of embryonic and induced pluripotent stem cells. *Cell Stem Cell*. 2011;8:309-317
4. Price AN, Cheung KK, Lim SY, Yellon DM, Hausenloy DJ, Lythgoe MF. Rapid assessment of myocardial infarct size in rodents using multi-slice inversion recovery late gadolinium enhancement cmr at 9.4t. *J Cardiovasc Magn Reson*. 2011;13:44
5. Heiberg E, Sjogren J, Ugander M, Carlsson M, Engblom H, Arheden H. Design and validation of segment--freely available software for cardiovascular image analysis. *BMC Med Imaging*. 2010;10:1
6. Riegler J, Cheung KK, Man YF, Cleary JO, Price AN, Lythgoe MF. Comparison of segmentation methods for mri measurement of cardiac function in rats. *J Magn Reson Imaging*. 2010;32:869-877

Cardiac Tissue Slice Transplantation as a Model to Assess Tissue-Engineered Graft Thickness, Survival, and Function

Johannes Riegler, Astrid Gillich, Qi Shen, Joseph D. Gold and Joseph C. Wu

Circulation. 2014;130:S77-S86
doi: 10.1161/CIRCULATIONAHA.113.007920
Circulation is published by the American Heart Association, 7272 Greenville Avenue, Dallas, TX 75231

Print ISSN: 0009-7322. Online ISSN: 1524-4539